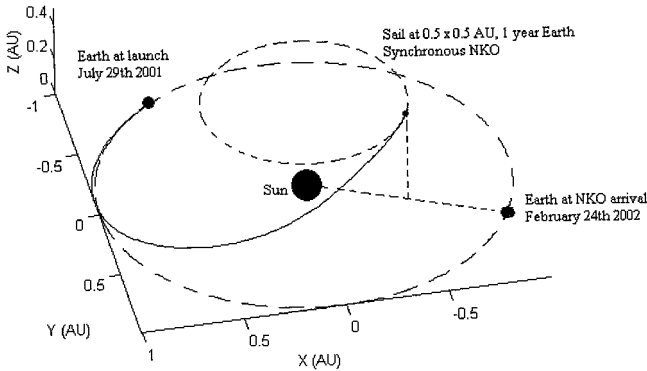
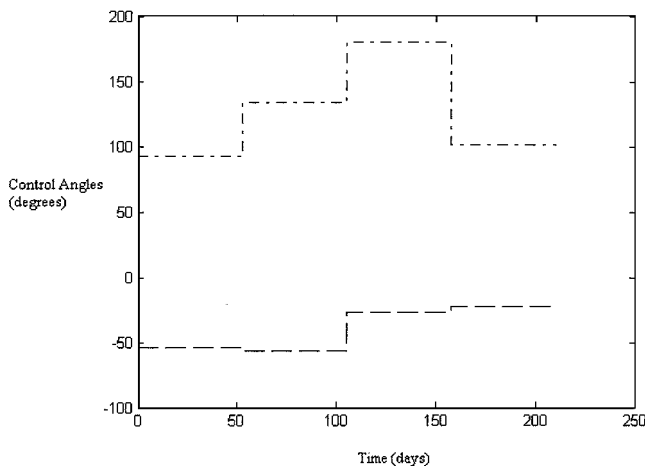


**Table 2** Sail lightness  $\beta$  as dependent on vertical displacement above ecliptic pole,  $z$ , and horizontal displacement from ecliptic pole,  $\rho$

$z$ , AU	$\rho$ , AU	$\beta$
0.2	0.9	0.43
0.5	0.5	0.88
0.7	0.3	0.97



**Fig. 2** Four-segment transfer to Earth synchronous  $0.5 \times 0.5$  AU, one-year NKO launched 29 July 2001.



**Fig. 3** Control angle history for transfer to Earth synchronous  $0.5 \times 0.5$  AU, one-year NKO: ---, cone angle; and - · -, clock angle.

stages of the transfer, the thrust was directed mostly in the opposite direction to the velocity vector; for the intermediate stage, the thrust is an almost entirely out-of-plane.

### Conclusions

A trajectory optimization tool has been developed which hybridized a GA with SQP. When applied to the difficult problem of preliminary mission planning for high-performance solar sail transfers to displaced NKO, it appeared to identify near-optimal trajectories with relative ease. The transfer time penalties (estimated from transfer time convergence as the number of segments was increased) appear acceptable even for a small number of segments (four or five). A small number of segments reduced the computational burden imposed by using a GA and would simplify attitude control in practice.

### Acknowledgment

The genetic algorithm was developed by D. L. Carroll of the University of Illinois.

### References

- <sup>1</sup>McInnes, C. R., *Solar Sailing: Technology Dynamics and Mission Applications*, Springer-Praxis Series in Space Science and Technology, Springer-Verlag, Berlin, 1999, pp. 171–228.

- <sup>2</sup>Walker, M. J. H., Ireland, B., and Owens, J., "A Set of Modified Equinoctial Orbit Elements," *Celestial Mechanics*, Vol. 36, 1985, pp. 409–419.

- <sup>3</sup>Bryson, A. E., Jr., and Ho, Y. C., *Applied Optimal Control*, Hemisphere, New York, 1975, pp. 42–69.

- <sup>4</sup>Goldberg, D. E., *Genetic Algorithms in Search, Optimization, and Machine Learning*, Addison Wesley Longman, Reading, MA, 1989.

- <sup>5</sup>Rauwolf, G. A., and Friedlander, A., "Near-Optimal Solar Sail Trajectories Generated by a Genetic Algorithm," American Astronautical Society/AIAA Astrodynamics Specialists Conf., AAS Paper 99-332, Aug. 1999.

- <sup>6</sup>Fowler, W. T., Crain, T., and Eisenreich, J., "The Influence of Coordinate System Selection on Genetic Algorithm Optimization of Low-Thrust Spacecraft Trajectories," American Astronautical Society/AIAA Spaceflight Mechanics Meeting, AAS Paper 99-130, Feb. 1999.

- <sup>7</sup>Coverstone-Carroll, V., Hartmann, J. W., and Mason, W. J., "Optimal Multi-Objective Low-Thrust Spacecraft Trajectories," *Computer Methods in Applied Mechanics and Engineering*, Vol. 186, 2000, pp. 387–402.

## Optimal Earth-Capture Trajectories Using Electric Propulsion

C. A. Kluever\*

University of Missouri-Columbia,  
Columbia, Missouri 65211

### Introduction

WITH the success of Deep Space 1, electric propulsion (EP) has become a viable propulsion option for performing interplanetary space missions.<sup>1</sup> One potential interplanetary application of EP is for the Earth-return leg of a sample return mission.<sup>2</sup> In this scenario, EP would eventually perform the capture maneuver from hyperbolic approach to a closed Earth orbit. It appears that research involving optimal EP capture trajectories, especially transfers involving hundreds of orbital revolutions, is somewhat limited. Battin<sup>3</sup> presented a feasible scheme for performing capture trajectories into a low lunar orbit with a variable low-thrust engine. Recently, Vadali et al.<sup>2</sup> demonstrated a Lyapunov feedback control law for performing a low-thrust capture into a high-altitude Earth elliptical orbit. In this Note, a new approach for computing optimal Earth-capture trajectories is presented. This approach joins numerically integrated trajectories with curve fits of universal low-thrust solutions to represent efficiently and accurately the complete capture phase. Numerical results are presented for minimum-propellant trajectories.

### System Model

The Earth-capture trajectory is governed by the following dynamic equations:

$$\dot{\mathbf{r}} = \mathbf{v} \quad (1)$$

$$\dot{\mathbf{v}} = -\frac{\mu \mathbf{r}}{r^3} + \mathbf{a}_p + \mathbf{a}_T \quad (2)$$

$$\dot{m} = \frac{-2\eta P}{(g I_{sp})^2} \quad (3)$$

where  $\mathbf{r}$  and  $\mathbf{v}$  are the position and velocity vectors of the spacecraft in an Earth-centered inertial (ECI) Cartesian frame,  $\mu$  is the Earth gravitational constant,  $\mathbf{a}_p$  is an acceleration vector due to perturbations, and  $\mathbf{a}_T$  is the thrust acceleration vector. Equation (3) defines the mass loss due to the low-thrust engine where  $m$  is spacecraft

Received 21 August 2001; revision received 17 January 2002; accepted for publication 17 January 2002. Copyright © 2002 by the American Institute of Aeronautics and Astronautics, Inc. All rights reserved. Copies of this paper may be made for personal or internal use, on condition that the copier pay the \$10.00 per-copy fee to the Copyright Clearance Center, Inc., 222 Rosewood Drive, Danvers, MA 01923; include the code 0731-5090/02 \$10.00 in correspondence with the CCC.

\*Associate Professor, Mechanical and Aerospace Engineering Department. Associate Fellow AIAA.

mass,  $P$  is input power to the EP system,  $\eta$  is engine efficiency,  $g$  is Earth gravitational acceleration, and  $I_{sp}$  is specific impulse. Perturbation vector  $\mathbf{a}_p$  in Eq. (2) accounts for Earth oblateness ( $J_2$ ) effects and lunar and solar gravitational acceleration. Thrust acceleration  $\mathbf{a}_T$  in the ECI frame is calculated by transforming the thrust acceleration components in a local-vertical/local-horizontal (LVLH) frame:

$$\hat{\mathbf{a}}_T = \frac{2\eta P}{mgI_{sp}} [\sin \alpha \cos \beta \quad \cos \alpha \cos \beta \quad \sin \beta]^T \quad (4)$$

Thrust direction in the LVLH frame is defined by the pitch  $\alpha$  and yaw  $\beta$  angles. Pitch is measured from the local horizon to the projection of the thrust vector onto the orbit plane, and yaw is measured from the orbit plane to the thrust vector.

The initial phase of the Earth-capture trajectory is computed through direct numerical integration of Eqs. (1–3) with a fixed-step, fourth-order Runge–Kutta method. However, the latter phase of the capture will involve hundreds of orbital revolutions before the spacecraft spirals down to the desired low-Earth-target orbit. Utilizing curve fits of low-thrust solutions eliminates the significant computational burden of computing the latter spiral stage. Perkins<sup>4</sup> developed universal solutions for low-thrust planar spiral transfers with a constant, continuous thrust force aligned with the velocity vector, that is, tangent steering. Defining the central body gravitational parameter, initial circular orbit radius, and thrust-to-weight ratio scales these dimensionless universal solutions. Perkins's solutions for dimensionless velocity magnitude  $V$ , flight-path angle  $\gamma$ , and dimensionless time parameter  $T$  are presented in Fig. 1 with dimensionless radial distance  $R$  as the independent variable. Following Perkins,<sup>4</sup> the dimensionless radius  $R$  is

$$R = (r_{\text{spiral}}/r_c) f^{\frac{1}{2}} \quad (5)$$

where  $r_{\text{spiral}}$  is the radial distance on the unwinding spiral,  $r_c$  is the initial circular radius, and  $f$  is the thrust-to-weight ratio. Dimensional values of velocity magnitude and spiral time to the point on the unwinding (or, inward winding) spiral can be computed from the interpolated values of  $V$  and  $T$  (which are obtained from curve fitting Fig. 1):

$$v_{\text{spiral}} = V v_c f^{\frac{1}{2}} \quad (6)$$

$$t_{\text{spiral}} = (T + f^{-\frac{1}{2}} - 0.809)(r_c/v_c) f^{-\frac{3}{2}} \quad (7)$$

Dimensionless time parameter,  $T = t_{\text{spiral}} - t_{\text{escape}}$ , is the time beyond local escape conditions. The dashed vertical line in Fig. 1 indicates the universal values of dimensionless radius  $R$ , velocity  $V$ , and flight-path angle  $\gamma$  for escape conditions, that is,  $T = 0$ . Flight-path angle on the spiral  $\gamma_{\text{spiral}}$  is obtained by simply curve fitting the data in Fig. 1 with  $R$  as the independent variable. If an inward (capture) spiral trajectory is desired, then the flight-path angle from the curve fit is set as a negative value.

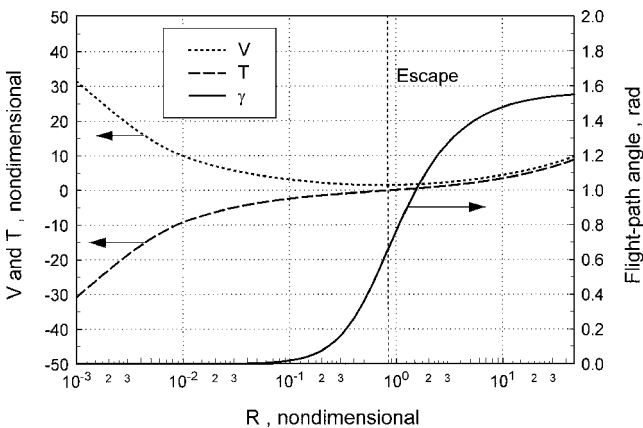


Fig. 1 Universal low-thrust trajectory parameters using Perkins's<sup>4</sup> approximation.

## Trajectory Optimization

The optimal control problem for the Earth-capture maneuver is stated as follows: Obtain the optimal pitch and yaw steering angles  $\alpha^*(t)$  and  $\beta^*(t)$ , for  $0 \leq t \leq t_1$ , and the simulation end time  $t_1$ , that minimize the performance index

$$J = \frac{2\eta P}{(gI_{sp})^2} (t_1 + t_{\text{spiral}}) \quad (8)$$

subject to Eqs. (1–3), with initial conditions

$$\mathbf{r}(0) = \mathbf{r}_0, \quad \mathbf{v}(0) = \mathbf{v}_0, \quad m(0) = m_0 \quad (9)$$

and the constraints

$$v(t_1) - v_{\text{spiral}} = 0 \quad (10)$$

$$\gamma(t_1) - \gamma_{\text{spiral}} = 0 \quad (11)$$

$$i(t_1) - i_{\text{LEO}} = 0 \quad (12)$$

The goal is to minimize the total propellant mass required for the low-thrust transfer to the desired low Earth orbit (LEO). Inward spiral time  $t_{\text{spiral}}$  is computed using Eq. (7), once  $T$  is obtained from curve fitting Fig. 1 with  $R$  determined by Eq. (5) and  $r_{\text{spiral}} = r(t_1)$ . Constraints (10) and (11) enforce a match between the end of the simulated trajectory and curve fits of the inward-spiral velocity [Eq. (6)] and flight-path angle, respectively. Constraint (12) requires that the orbital inclination  $i(t_1)$  at the end of the numerically simulated capture match the desired inclination of the LEO (recall that Perkins's<sup>4</sup> universal solutions are for planar transfers only).

Numerical solutions of the minimum-propellant problem are obtained by using a direct trajectory optimization method. The optimal control problem is replaced by a nonlinear programming problem, which is solved by using sequential quadratic programming (SQP), a constrained parameter optimization method. The SQP code used here is NPSOL, which uses finite differences to compute gradient information.<sup>5</sup> Time histories of pitch and yaw angles are parameterized by linear interpolation through a set of discrete nodes equally spaced along the time axis,  $0 \leq t \leq t_1$ . Therefore, the pitch and yaw control nodes and end time  $t_1$  are the NPSOL optimization variables. Three NPSOL equality constraints enforce trajectory constraints (10–12).

## Results

The initial condition for the Earth-capture trajectory is taken from the latter stage of a minimum-propellant Mars–Earth transfer, which could be the return phase of a low-thrust sample return mission. Initial Earth-relative  $\mathbf{r}$  and  $\mathbf{v}$  vectors (for the Earth capture problem) are determined by subtracting the Earth's position and velocity vectors from the spacecraft's heliocentric position and velocity vectors near the end of the Mars–Earth trajectory. The initial Earth-relative state is  $\mathbf{r}_0 = [-1.9376(10^5) \quad -9.6272(10^5) \quad -1.0861(10^6)]^T$  km and  $\mathbf{v}_0 = [0.1924 \quad 0.6384 \quad 0.6866]^T$  km/s, respectively, that place the spacecraft beyond the fictitious sphere of influence. Calendar date for this initial condition is 18 August 2014, and the initial orbital eccentricity and inclination are  $e = 1.0123$  and  $i = 53.28$  deg, with respect to the Earth. Initial flight-path angle is  $\gamma_0 = -85.79$  deg, for a nearly radial descent trajectory. Initial spacecraft mass is  $m_0 = 315$  kg. A 500-km altitude circular LEO with 28.5-deg inclination is the desired target orbit. The constant spacecraft system parameters are  $P = 3$  kW,  $\eta = 0.68$ , and  $I_{sp} = 3800$  s, which represent the current level of solar EP technology.

The optimal capture is obtained with NPSOL with a total of 33 optimization variables: 21 discrete control nodes for the pitch steering program, 11 nodes for yaw, and 1 optimization variable for simulation end time  $t_1$ . Minimum propellant mass is 62.1 kg, and the corresponding total capture time is 244.54 days, with  $t_1 = 47.40$  days and  $t_{\text{spiral}} = 197.14$  days. The optimal patch point between the numerically integrated trajectory and the inward spiral curve fit is at radius  $r(t_1) = 44.03$  Earth radii with velocity  $v(t_1) = 1.2130$  km/s, flight-path angle  $\gamma(t_1) = -7.92$  deg, and eccentricity  $e = 0.1425$ .

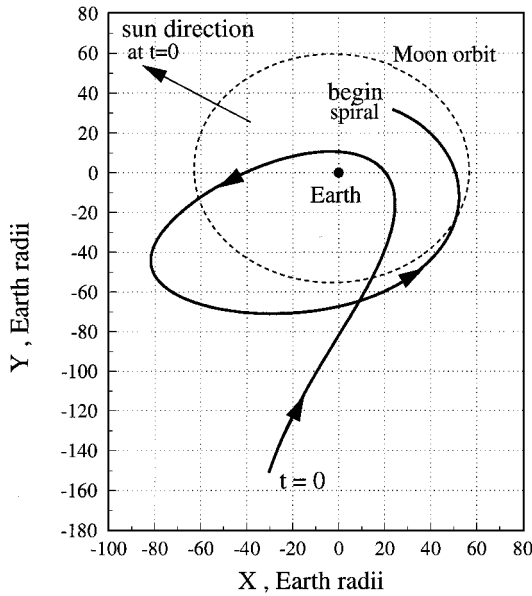


Fig. 2 Numerically integrated segment of the optimal Earth-capture trajectory.

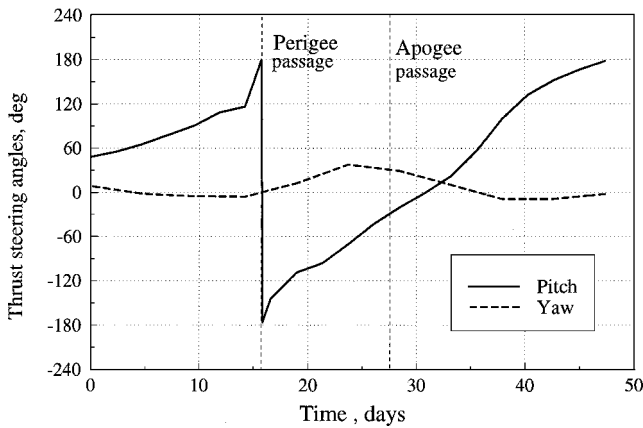


Fig. 3 Optimal thrust steering angles for the numerically integrated trajectory.

Figure 2 shows the numerically integrated phase of the capture trajectory (projected onto the equatorial plane) to the patch point. Note that the spacecraft completes about 1.5 revolutions about the Earth before reaching the proper conditions for the inward spiral. By comparison, the inward spiral from the patch point to LEO completes 851 revolutions about the Earth in 197.14 days. (An auxiliary numerical simulation of the planar spiral was used to ascertain the number of revolutions.) Figure 3 presents the optimal pitch and yaw steering programs for the simulated trajectory. The initial pitch angle is about 48 deg (above the horizon), which is required simultaneously to reduce energy and to increase both perigee and angular momen-

tum. Furthermore, pitch angle is nearly 180 deg at perigee passage (for decreasing semimajor axis and eccentricity) and -26 deg at apogee passage (for decreasing eccentricity). Pitch steering at the patch point is 178 deg, which is nearly opposite the velocity vector. Yaw steering for the required 24.8-deg plane change is most pronounced near apogee.

A more realistic representation of the planar inward spiral trajectory was obtained by considering periods of Earth shadow and null thrust, which are not accounted for by the Perkins<sup>4</sup> approximation. First, the inward spiral from the patch-point state was numerically simulated using Eqs. (1–3) with antitangent-thrust steering until the radius reached 6.5 Earth radii. Next, a direct trajectory optimization program<sup>6</sup> was used to obtain the minimum-time transfer from the state at 6.5 Earth radii to the target LEO. This optimization program utilizes orbital averaging and blended optimal steering laws, and accounts for Earth-shadow and oblateness effects (see Ref. 6 for details). The resulting inward spiral time was found to be 228 days, which is nearly 31 more days than the curve-fit (continuous-thrust) solution. However, the total propellant load for the full numerical simulation (with Earth shadow) is 63.1 kg, which is only 1.6% greater than the propellant mass from the trajectory using the curve-fit approximation.

## Conclusions

A new approach for computing minimum-propellant, Earth-capture EP trajectories has been presented. The initial phase of the trajectory (from hyperbolic approach to capture) is numerically computed using the combined gravity fields of the Earth, sun, and moon. The solution method eliminates the computational burden of simulating the hundreds of near-circular revolutions of the inward spiral transfer to LEO by utilizing curve fits of universal low-thrust solutions. This strategy requires few optimization variables and readily yields a minimum-propellant solution. A full numerical simulation of the inward spiral transfer (with Earth-shadow effects and  $J_2$ ) exhibits a very good match with the curve-fit results in terms of propellant load. Furthermore, the resulting optimal thrust steering program for the capture phase exhibits a smooth profile with linear segments, which may simplify implementing an onboard guidance strategy.

## References

- Rayman, M. D., Varghese, P., Lehman, D. H., and Livesay, L. L., "Results from the Deep Space 1 Technology Validation Missions," *Acta Astronautica*, Vol. 47, Nos. 2–9, 2000, pp. 475–487.
- Vadali, S. R., Aronwilairut, K., and Braden, E., "A Hybrid Trajectory Optimization Technique for the Mars Sample Return Mission," American Astronautical Society, Paper AAS 01-466, Aug. 2001.
- Battin, R. H., *Astronautical Guidance*, 1st ed., McGraw-Hill, New York, 1964, pp. 344–354.
- Perkins, F. M., "Flight Mechanics of Low-Thrust Spacecraft," *Journal of the Aerospace Sciences*, Vol. 26, No. 5, 1959, pp. 291–297.
- Gill, P. E., Murray, W., Saunders, M. A., and Wright, M. H., "User's Guide for NPSOL (Version 4.0): A Fortran Package for Nonlinear Programming," Systems Optimization Lab., Stanford Univ., Stanford, CA, Jan. 1986.
- Kluever, C. A., and Oleson, S. R., "Direct Approach for Computing Near-Optimal Low-Thrust Earth-Orbit Transfers," *Journal of Spacecraft and Rockets*, Vol. 35, No. 4, 1998, pp. 509–515.